Synergistically Improved Anti-tumor Efficacy by Co-delivery Doxorubicin and Curcumin Polymeric Micelles

Jinling Wang, Wenzhuan Ma, Pengfei Tu*

P-gp mediated drug efflux has been recognized as a major obstacle limiting the success of cancer chemotherapy. To overcome this issue, doxorubicin (DOX) and curcumin (Cur; P-gp inhibitor and apoptosis inhibitor) co-encapsulated pegylated polymeric micelles ((DOX+Cur)-PMs) were designed, prepared and characterized to simultaneously deliver chemotherapeutic drug and multidrug resistance (MDR) modulator to tumor sites. The (DOX+Cur)-PMs were spherical nano-size particle, with a loading content of 6.83%, and high colloidal stability. Co-delivery micelles exhibited excellent cytotoxicity by reversing MDR, promoting cellular uptake and enhancing cellular apoptosis in MCF7/Adr cells. The tumor growth inhibitory effect of (DOX+Cur)-PMs in 4T1-bearing mice was more effective compared with the combination solution of DOX and Cur and even DOX-PMs. In conclusion, simultaneous delivery of DOX and Cur by (DOX+Cur)-PMs has been demonstrated to be a promising approach for overcoming MDR and improving antitumor efficacy.

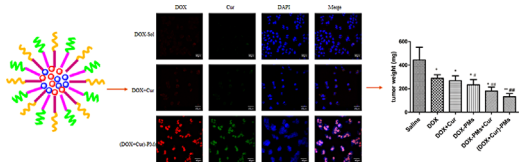

1. Introduction

Multidrug resistance (MDR) has been recognized as a major obstacle limiting the success of cancer chemotherapy.[1] Among multiple resistance mechanisms, adenosine triphosphate (ATP) binding cassette transporters mediated drug efflux is most commonly encountered in clinic.[2] Doxorubicin (DOX), an anthracycline antibiotic, is one of the most effective chemotherapy drugs in clinical cancer therapy. However, the clinical application of DOX has been hindered for MDR and systemic toxic side-effects, including cardiotoxicity and bone marrow suppression. Therefore, it is very necessary to find effective approaches to overcome MDR and reduce side effects of DOX for chemotherapy.

Prof P. Tu, J. Wang, W. Ma
Modern Research Center for Traditional Chinese Medicine, Beijing University of Chinese Medicine, Beijing 100029, PR China
Fax: (86)-10-82802750; E-mail: pengfeitu@163.com
W. Ma
School of Chinese Materia Medica, Beijing University of Chinese Medicine, Beijing 100102, PR of China

In the past decades, several synthetic small molecules and antibodies targeted against MDR protein have been simultaneously used with chemotherapy agents, but they are limited in clinic because of severe toxicity and low stability.[3] Nowadays, more attention has been focused on Nature herbs, which could be safe with no side effects, strengthen immunity and improve the sensitivity of chemotherapy. More attractively, synergistic combination therapy with natural chemosensitizers is emerging as a promising strategy for conquering MDR and reducing side effects of chemotherapeutic medicine.

Curcumin (Cur), a natural polyphenol constituent of *Curcuma longa*, exhibits a wide range of therapeutic activities, such as anti-oxidant, antitoxic, anti-inflammatory, antimicrobial, and antitumor effects.[4] Despite of the excellent pharmacological properties, Cur is an ideal chemosensitizer to downregulate multidrug resistance proteins,[5,6] and inhibit cancer cell proliferation through inhibition of human epidermal growth factor receptor-2 (HER2) activity and nuclear factor kappa B (NF-κB) activation.[7,8] Meanwhile, Cur has a potential of myocardial protective effect and no systemic side effects to human organs even at high doses.[9,10] Recently, many studies have

DOI: 10.1002/mabi.201500043

proposed that co-delivery of DOX and Cur could achieve a synergistic therapeutic effect on tumor therapy.[11] However, Cur has been inactive in clinic use, because of water insolubility and poor bioavailability.[4,7,12] Therefore, a combination of free DOX and free Cur could not have any obvious synergistic effect because of rapid elimination of the drugs in vivo. Currently, several co-delivery systems of DOX and Cur, including liposomes and nanoparticles, have been proposed to simultaneously deliver Cur and DOX to tumor sites, and displayed better antitumor efficacy and lower systemic toxicity compared with DOX solution.[4,13–15] However, DOX and Cur co-delivery micellar system was less studied.

Polymeric micelles (PMs) have been widely applied as a promising nanocarrier to circumvent MDR and enhance the chemotherapy effects. PMs could self-assemble in aqueous medium with biodegradable amphiphilic copolymer to form a core-shell structure, where hydrophobic drugs were entrapped into a hydrophobic inner core to improve drug stability. The hydrophilic outer shell of PMs has the ability to increase the solubility and prolong circulating half-time of encapsulated hydrophobic drugs. Moreover, PMs could escape from the recognition of reticulo-endothelial system (RES), because hydrophilic shell of PMs reduces protein adsorption on micelles.[16] Meanwhile, due to the nano-size of PMs, PMs could selectively accumulate in tumor sites and improve antitumor efficacy, mainly due to enhanced permeability and retention effects (EPR).[17]

D-α-Tocopheryl polyethylene glycol succinate (TPGS), approved by Food and Drug Administration (FDA) as a safe pharmaceutical adjuvant, has attracted more attention for the treatment of drug resistant in chemotherapy.[18] Furthermore, TPGS could inhibit P-gp efflux pump to reversal MDR, enhance cellular uptake and improve the anticancer effects.[18,19] TPGS2000 (d-a-tocopheryl polyethylene glycol succinate 2000), as an analog of TPGS, has a lower critical micelle concentration (CMC; 0.022 mg mL^{-1}) than TPGS (0.2 mg mL^{-1}) and could overcome MDR by inhibiting P-gp.[20] However, it was scarcely used to form co-delivery micelles of dual agents.

In the present study, mixed micelles incorporated with DOX and Cur (P-gp inhibitor and apoptosis inhibitor) were prepared with two diblock polymers, TPGS2000 and PEG2000-DSPE, to simultaneously delivery dual agents for overcoming MDR and improving antitumor effects of DOX. The physicochemical properties of micelles were investigated. The efficacy of DOX and Cur co-encapsulated micelles ((DOX+Cur)-PMs) on reversal MDR was evaluated in MCF7 and MCF7/Adr cells in vitro, and the mechanism of cellular uptake was also investigated in MCF7/Adr cells. Furthermore, the synergistic antitumor effect of (DOX+Cur)-PMs was evaluated in 4T1 bearing Balb/C mice in vivo. The prepared (DOX+Cur)-PMs are expected be a promising vehicle to enhance the antitumor efficacy and reduce systemic toxic.

2. Experimental Section

2.1. Materials

DOX · HCl was obtained from Beijing Huafeng Ynited Technology Co., Ltd (Beijing, China). Cur was purchased from Sigma-Aldrich (St. Louis, MO, USA). Di-tocopherol polyethylene glycol 2000 succinate (TPGS2000) was synthesized by our group. 1,2-distearoyl-sn-glycero-3-phosphoethanolamine-*N*-[methoxy-(polyethylene glycol)-2000] (PEG2000-DSPE) was obtained from Xi'an Ruixi Biological Technology Co., Ltd. (Xi'an, Shanxi, China). Roswell Park Memorial Institute (RPMI) 1640 medium and fetal bovine serum (FBS) were obtained from Gibco (BRL, Gaithersburg, MD, USA). 3-(4,5-dimethyl-2-thiazolyl)-2,5-diphenyl-2*H*-tetrazolium bromide (MTT) and trypsin were also purchased from Sigma-Aldrich (St. Louis, MO). All solvents used in this investigation were of HPLC grade.

2.2. Animals

Sprague-Dawley rats weighing 220 g ± 20 g and female Balb/c mice aged 5 weeks about 20 g were purchased from Beijing Vita River Company. All animal experiments were performed in accordance with guidelines for the Use and Care of Animals approved by the Beijing University of Chinese medicine Committee of Ethics. The animals were maintained at animal care facility for at least 3 d with fresh diet and water daily before experiments.

2.3. Preparation and Characterization of Co-delivery DOX-Cur Micelles

Co-delivery micelles of (DOX+Cur)-PMs were prepared via solvent evaporation method. Briefly, DOX · HCl (5 mg) was reacted with a two molar excess of triethylamine in methanol to obtain doxorubicin free base (DOX). Then, DOX, 5 mg of Cur, 100 mg of TPGS2000 and 20 mg of PEG2000-DSPE were dissolved in methanol solution under mild stirring. The organic solvent was removed under reduced pressure by rotary vacuum evaporation. The film of drug-polymer was hydrated in normal saline with stirring at 37 °C for 4 h, followed by centrifugation (12 000 rpm, 10 min) and filtration through a 0.22 μm filters to obtain (DOX+Cur)-PMs. The DOX-PMs and blank micelles were prepared in the same way, but without DOX or Cur. The DOX-PMs+Cur were prepared via physical mixing DOX-PMs and Cur-Sol.

Size distribution and zeta potential of (DOX+Cur)-PMs were determined by dynamic light scattering (DLS) using a Zetasizer (Nano ZS 90, Malvern Co., UK). Measurements were repeated in triplicate.

The morphology of (DOX+Cur)-PMs was evaluated on transmission electron microscopy (TEM, Tecnai 20 200 kV, FEI). The diluted micelles were placed on a copper grid and negative stained with 1% uranyl acetate before observation by TEM.

Meanwhile, the colloidal stability of (DOX+Cur)-PMs was evaluated to measure the changes of size and zeta potential after incubation with 1%, 5% and 10% BSA at 37 °C for 24 h.

For determination of encapsulation efficiency (EE) and drug-loading (DL), (DOX+Cur)-PMs, (DOX+Cur)-PMs or freeze-dried (DOX+Cur)-PMs were diluted with methanol and ultrasonic energy was used to destroy the micelles, and the content of DOX or Cur in micelles was analyzed by HPLC. Encapsulation efficiency was calculated by the ratio of encapsulated DOX or Cur in micelles to the amount of DOX or Cur added in. Drug-loading was calculated as the percentage of the amount of drug loaded in micelles to the weight of lyophilized drug-loaded micelles. The chromatographic separations were accomplished on Eclipse XDB-C18 column (4.6×250 mm, 5 μm, Agilent) with mobile phase of methanol, 3 mm monopotassium phosphate, acetic acid (58:42:0.5, v/v/v) at a detection wavelength of 227 nm.

The release profiles of DOX and Cur from (DOX+Cur)-PMs were determined by a modified dialysis method. (DOX+Cur)-PMs were sealed in dialysis bags of molecular weight cut-off (MWCO) of 14 000 and immersed in phosphate buffer (pH 7.4). At desired time intervals, 1 mL of release medium was withdrawn and analyzed by HPLC as described above. Experiments were carried out in triplicate.

2.4. Cell Culture

Dox-sensitive (MCF-7) and DOX-resistant (MCF-7/Adr) human breast carcinoma cells were purchased from Nanjing Kaiji Biotech. Ltd. Co. (Nanjing, China). Cells were cultured in RPMI-1640 medium with 10 vol% FBS and 1% penicillin-streptomycin with 5% CO_2 at 37 °C. In addition, MCF-7/Adr cells were incubated in medium with 1 μg mL^{-1} DOX. The cells were sub-cultured with 0.25% trypsin when reaching 80–90% confluence.

2.5. In Vitro Cytotoxicity

MCF-7 and MCF-7/Adr cells were seeded at a density of 5×10^4 cells/well/0.1 mL 1640 culture medium and attached for 24 h in 96-well plates. Then, the cells were incubated with DOX, DOX+Cur, DOX-PMs, DOX-PMs+Cur, or (DOX+Cur)-PMs at equivalent DOX concentration of 0.01, 0.1, 0.2, 0.4, 0.8, or 1 μg ml^{-1} for MCF-7 cells for 48 h, and 0.5, 1, 2, 5, 10, 20, or 40 μg ml^{-1} for MCF-7/Adr cells for 48, 72 or 96 h incubation, respectively. Then cell growth inhibition rate was calculated by MTT.

2.6. Cellular Uptake and Efflux

MCF-7/Adr cells were seeded in 24-well plates at a density of 1×10^5 cells per well for 24 h attachment. Cells were incubated with DOX, DOX+Cur, DOX-PMs, DOX-PMs+Cur, or (DOX+Cur)-PMs at an equivalent DOX concentration of 10 μg ml^{-1} for 2 h or 4 h incubation. Then, cells were washed with cold phosphate-buffered saline (PBS) three times, trypsinized and harvested in PBS. The fluorescent intensity of DOX in cells was measured by fluorescence-activated cell sorting (FACS).

To investigate the efflux effects of DOX preparations, MCF-7/Adr cells were cultured in 24-well plates for 24 h. MCF7/Adr cells were treated with DOX, DOX+Cur, DOX-PMs, DOX-PMs+Cur, and (DOX+Cur)-PMs at an equivalent DOX concentration of 10 μg ml^{-1} for 2 h. Then, cells were washed with PBS twice, and incubated with fresh medium for another 1 h and 2 h. After that, cells were trypsinized, and harvested. The intracellular fluorescent intensity of DOX was measured by FACS.

2.7. Subcellular Localization

To visualize subcellular localization of DOX samples in cells, MCF7/Adr cells were seeded onto cover-slips for 24 h pre-incubation. Then, cells were washed with Hanks' balanced salt solution (HBSS) and co-cultured with DOX, DOX+Cur or (DOX+Cur)-PMs for 1 h and 3 h, respectively. Afterwards, cells were washed with cold PBS twice, fixed with 4% paraformaldehyde for 10 min, and counterstained to mark cell nucleus by 4',6-diamidino-2-phenylindole (DAPI). In addition, cells were mounted on slides and visualized by confocal laser scanning microscope (Olympus, Japan).

2.8. Endocytosis Mechanism

The endocytotic pathway of (DOX+Cur)-PMs in MCF7/Adr cells was investigated with specific endocytosis inhibitors and detected by FACS. Initially, MCF7/Adr cells were seeded in 24-well plates for 24 h. Then, cells were washed and pre-incubated with chlorpromazine (10 μg mL^{-1}), quercetin (40 μg mL^{-1}), indomethacin (100 μg mL^{-1}), β-cyclodextrin (2 mg mL^{-1}) for 1 h at 37 °C. After that, cellular monolayers were incubated with the combination of (DOX+Cur)-PMs and corresponding endocytosis inhibitors for an additional 1 h at 37 °C. Cells, treated with micelles only, were used as a control. Meanwhile, cells, pre-incubated for 1 h at 4 °C and then cultured with (DOX+Cur)-PMs at 4 °C for another 1 h, were employed to investigate energy-mediated endocytosis compared with that at 37 °C. After co-incubation, MCF7/Adr cells were washed with PBS, digested and harvested. Finally, the obtained living cells were immediately detected by FACS.

2.9. Apoptosis

MCF7/Adr cells were seeded in 24-well plates at a density of 1×10^5 cells per well. After 24 h incubation, cells were incubated with DOX, DOX+Cur, DOX-PMs, DOX-PMs+Cur, or (DOX+Cur)-PMs at an equivalent DOX concentration of 10 μg ml^{-1} for 48 h. Then cells were trypsinized, washed with cold PBS twice and harvested. Then, cells were stained with Annexin V-FITC (fluorescein-isothiocyanate labelled) and PI for 10 min at room temperature in the dark. Afterwards, binding buffers were added and the samples were analyzed by FACS.

2.10. Pharmacokinetics in Vivo

Male Sprague-Dawley rats were randomly divided into five groups (n=5). Rats were fasted 12 h with free access to water before dosing. Then, DOX, DOX+Cur, DOX-PMs, DOX-PMs+Cur, or (DOX+Cur)-PMs were intravenously administrated to rats at a dose of 5 mg kg^{-1} DOX, respectively. After administration, 0.2 mL of blood samples were collected by puncture the retro-orbital sinus at 0.033, 0.083, 0.167, 0.33, 0.5, 1, 2, 4, 6, 8, 10, 12, 24, 48, and 96 h. Plasma samples were obtained by centrifugation at 4000 × g for

10 min immediately after sampling and analyzed by UPLC-MS/MS after precipitation by methanol.

2.11. Antitumor Effects in Vivo

Female Balb/c mice bearing 4T1 tumor were randomly divided into six groups (n=6). When tumors reached about 100 mm^3, mice were intravenously administered with DOX-Sol, DOX+Cur, DOX-PMs, DOX-PMs+Cur or (DOX+Cur)-PMs at a dose of DOX 10 mg kg^{-1} by tail vein every other two days, respectively, with the group administered with saline as a control. Body weights and tumor volumes were measured every two days after administration. The tumor volume was calculated as the equation: $V = ab^2/2$, where a was major axis and b was minor axis measured by slide caliper. At the end of the experiment, mice were sacrificed, and tumors were excised and weighted.

2.12. Statistical Analysis

Results were expressed as means ± SD (standard deviation). A student's t-test or one-way analysis of variance (ANOVA) was applied to test for significance in the experiments. Statistical differences were considered significant at $P < 0.05$ and very significant at $P < 0.01$.

3. Results and Discussion

3.1. Preparation and Characterization of (DOX-Cur)-PMs

In this work, co-delivery DOX and Cur polymeric micelles were developed to improve antitumor effects and decrease side effects of DOX.

TPGS2000 and PEG2000-DSPE could self-assemble in aqueous medium to form core-shell structure micelles and encapsulate hydrophobic drugs of DOX and Cur in the inner core. (DOX+Cur)-PMs displayed a narrow particle size of 13.76 ± 0.14 nm and a neutral zeta potential of 0.42 ± 0.19 mV determined by DLS (Figure 1A and 1B). Micelles were spherical shape with good monodispersity visualized by TEM in Figure 1E. Nano-size particles of (DOX+Cur)-PMs could be beneficial for targeting tumor sites through EPR effects. Moreover, a neutral charge of micelles, caused by PEG shell, was more conductive to avoid micelles being cleared by kidneys infiltration (<10 nm) and RES (>100 nm).[21]

Encapsulation efficiency of DOX and Cur in (DOX+Cur)-PMs were 92.9 ± 0.78% and 97.42 ± 0.02%, respectively, which indicated that both DOX and Cur were well packaged in the hydrophobic core of micelles. Moreover, the loading efficiency of drugs in (DOX-Cur)-PMs were 6.83%.

To characterize colloidal stability of (DOX+Cur)-PMs in aqueous 1%, 5%, and 10% bovine serum albumin (BSA) solution, size and zeta potential were evaluated (Figure 1C and 1D). Particle sizes were slightly increased with the increase of BSA concentrations and incubation times. Moreover, even if the concentration of BSA reached 10%, no visible precipitation was observed for micelles. Meanwhile, zeta potentials were decreased with the increase of BSA concentrations, which was due to the slight negative charge of BSA. Therefore, micelles were stable in BSA aqueous, and could maintain micellar structure integrity in blood circulation.

Cumulative release profiles of (DOX-Cur)-PMs were shown in Figure 1F. Approximately 56% of DOX and 27% of Cur were released from (DOX-Cur)-PMs within 24 h. The initial burst release was due to the diffusion of drugs at micellar surface, and then the drugs inside micellar inner core were gradually released. Unfortunately, cumulative release of DOX within 24 h was higher than Cur, which may be due to stronger hydrophobicity of Cur than DOX.

3.2. Cytotoxicity in Vitro

Cytotoxicity of DOX, Cur, DOX+Cur, DOX-PMs, DOX-PMs+Cur, and (DOX+Cur)-PMs was investigated in sensitive MCF-7 and resistant MCF-7/Adr cells by MTT assay. The growth inhibition profiles of DOX in various DOX formulations in MCF-7 for 48 h and MCF-7/Adr cells for 48, 72 and 96 h, are shown in Figure 2. In MCF-7 cells, due to the additional cytotoxicity of Cur, the cytotoxic effect of DOX+Cur was higher than DOX. Meanwhile, DOX-PMs, DOX-PMs+Cur and (DOX+Cur)-PMs had the similar cytotoxicity, but exhibited significantly higher cytotoxicity compared with DOX and DOX+Cur in solution in MCF-7 cells, which indicated that co-administration of DOX and Cur in micelles would synergistically enhance therapeutic efficiency in vitro.

Furthermore, Cur combined with DOX solution enhanced the growth inhibitory effect of DOX, compared with single DOX-Sol in P-gp overexpressed MCF-7/Adr cells, which was mainly because Cur was an inhibitor of NFκB as well as a downregulator of MDR transporters. DOX-PMs, DOX-PMs+Cur and (DOX+Cur)-PMs exhibited significantly higher cytotoxicity compared with DOX-Sol and DOX+Cur with the prolongation of incubation times, implying that DOX encapsulated in micelles could be easily permeated into resistant MCF-7/Adr cells, enhance the cytotoxicity of DOX and reverse the MDR. Moreover, the growth inhibition of dual-drug loaded (DOX+Cur)-PMs was slightly higher than that of DOX-PMs and DOX-PMs+Cur, showing that MDR could be further overcome by co-encapsulated chemotherapeutic drugs and reversal agents in nanoparticles.

3.3. Cellular Uptake and Efflux

Cellular uptake of DOX was carried out in P-gp overexpressed MCF-7/Adr cells quantitatively and qualitatively

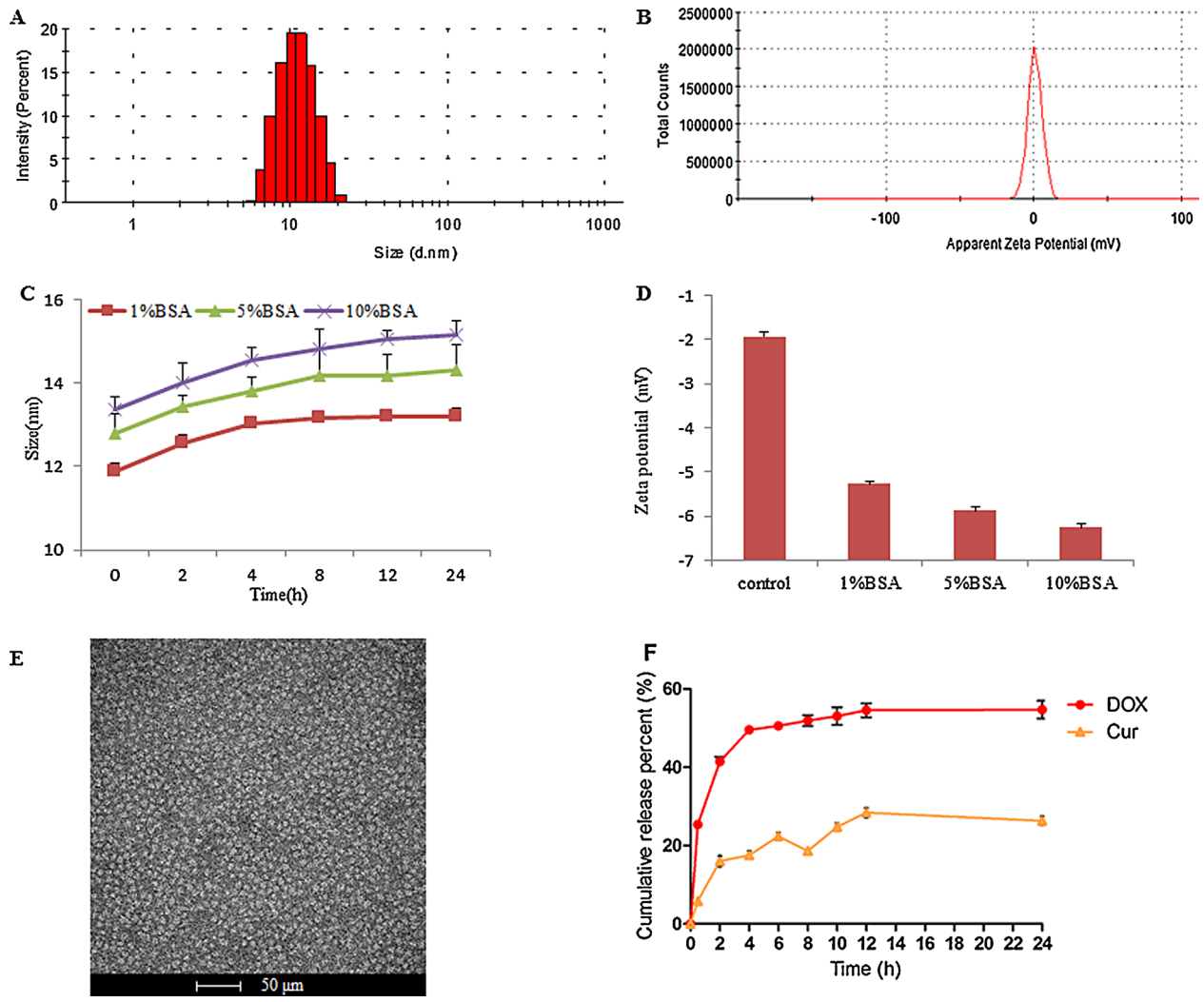

Figure 1. (A) Size distribution and (B) zeta potential of (DOX+Cur)-PMs determined by DLS, (C) Colloidal stability of (DOX+Cur)-PMs in 1%, 5% and 10% BSA aqueous after incubation for 24 h, (D) Zeta potential changes of (DOX+Cur)-PMs in 1%, 5% and 10% BSA aqueous at 37 °C for 24 h, (E) TEM image of (DOX+Cur)-PMs (scale bar =50 μm), (F) Cumulative release profiles of DOX and Cur from (DOX+Cur)-PMs in pH 7.4 PBS for 24 h (n = 3, mean ± SD).

by FACS and CLSM, respectively. For quantitative research, cellular fluorescence intensity of DOX in all DOX formulations was increased with the prolongation of incubation time (Figure 3A). The amount of DOX-Sol accumulated in MCF7/Adr cells was very low, mainly due to P-gp efflux effect in MCF-7/Adr cells. However, DOX+Cur improved cellular uptake of DOX-Sol, which was contributed to the P-gp inhibitory effect by the addition of Cur. Interestingly, cellular uptake of DOX was significantly enhanced by DOX-PMs, DOX-PMs+Cur and (DOX+Cur)-PMs at both 2 h and 4 h, and the uptake amount was extremely increased with the incubation time extended from 2 h to 4 h. Enhanced uptake of micelles was mainly owing to the nano-size of micelles and more easier to penetrate into resistant cells. Therefore, DOX encapsulated in micelles could enhance cellular uptake and reverse MDR. Moreover, cells treated with (DOX+Cur)-PMs showed higher internalization of DOX in comparison with DOX-PMs and DOX-PMs+Cur. It was as a result of the synergistic effects of co-delivery of DOX and Cur in micelles, which was due to the simultaneous release of DOX and Cur, reducing the efflux of DOX by Cur and leading to higher intracellular concentration of DOX. That also was the reason of free Cur in solution unable to enhance the cellular uptake and cytotoxicity of DOX-PMs.

Cellular uptake of DOX-Sol, DOX+Cur and (DOX+Cur)-PMs was also imaged by CLSM, as shown in Figure 4, and the fluorescence intensities of DOX and Cur in DOX formulations were all increased with time extension. However, less fluorescence intensity of DOX in DOX-Sol was observed

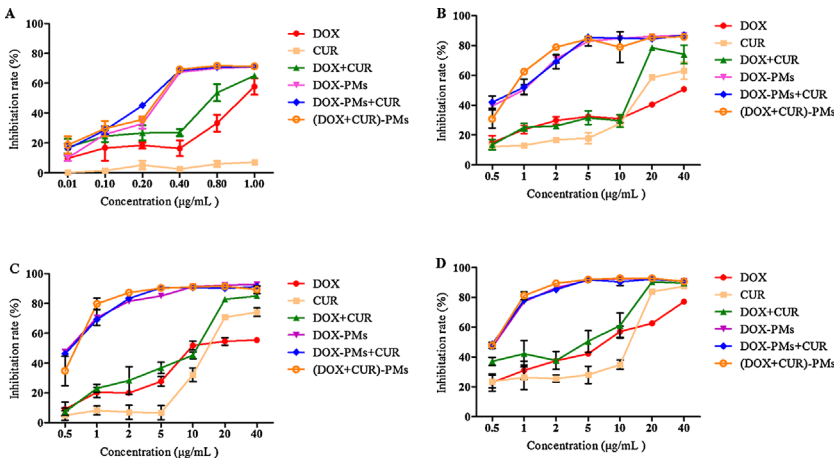

Figure 2. Cytotoxicity of DOX-formulations in MCF7 for 48 h (A) and MCF7/Adr cells for 48 h (B), 72 h (C) and 96 h (D), respectively. (n = 3, mean ± SD).

after 1 h or 3 h of co-incubation. However, the fluorescence intensity of DOX in combined DOX+Cur solution was increased to a certain extent compared with DOX-Sol after 3 h incubation, which once again vividly proved that Cur could synergistically improve cellular accumulation of DOX. The localization of DOX in cells treated with DOX+Cur was almost at the edge of cell nucleus. Furthermore, (DOX+Cur)-PMs significantly enhanced cellular uptake of DOX compared with DOX-Sol and DOX+Cur group after 1 h or 3 h incubation, which was in accordance with the results of FACS. Subcellular localization of (DOX+Cur)-PMs was almost in nucleus. In consequence, the cellular uptake of DOX in DOX formulations was all time-dependent, and (DOX+Cur)-PMs could significantly improve the intracellular accumulation of DOX and lead to greater cytotoxicity.

In cellular efflux study, the amount of DOX retained in MCF-7/Adr cells was decreased with time prolongation, as a result of P-gp pumping anticancer drugs out of cells (shown in Figure.3B). Mean fluorescence intensity of DOX+Cur in MCF-7/Adr cells was also decreased with incubation time extended, but the reduced degree was lower than DOX-Sol group. Surprisingly, intracellular amount of DOX was still significantly high in DOX-PMs, DOX-PMs+Cur and (DOX+Cur)-PMs, and the downward trends of drug efflux were slow, which showed that DOX encapsulated in micelles could reduce efflux and overcome the MDR. Meanwhile, the intracellular concentration of DOX in (DOX+Cur)-PMs was higher than DOX-PMs and DOX-PMs+Cur in cellular efflux, mainly due to the P-gp efflux inhibition effects by Cur after being released from micelles.

3.4. Endocytosis Mechanism

Polymeric micelles usually internalize into cells through endocytosis pathway, so specific endocytosis inhibitors were used to investigate endocytosis mechanism of prepared (DOX+Cur)-PMs. As shown in Figure 5, cellular uptake of DOX was markedly inhibited at 4 °C compared with 37 °C ($p < 0.01$), indicating that energy-dependent endocytosis pathway of (DOX+Cur)-PMs was involved. Furthermore, cellular uptake of (DOX+Cur)-PMs was decreased after co-incubation with β-cyclodextrin (inhibitor of lipid raft and caveolae- dependent endocytosis), [22] indomethacin (inhibitor of cyclooxygenase (COX) and caveolae-mediated endocytosis), [23] and quercetin (an inhibitor of caveolae- and clathrin-independent endocytosis), implying that caveolae-dependent endocytosis and caveolae- and clathrin-independent endocytosis were involved in the endocytosis mechanisms of (DOX+Cur)-PMs. However, chlorpromazine,[24] an inhibitor of CME, had no effects on the internalization of (DOX+Cur)-PMs. Therefore, enhanced cellular uptake of (DOX+Cur)-PMs was via energy-dependent, caveolae-dependent endocytosis and caveolae- and clathrin-independent endocytosis. In conclusion, co-delivery of DOX and Cur micelles (DOX+Cur)-PMs reversed MDR by two pathways: first, micelles were taken uptake into P-gp overexpressed cells by endocytosis and improved DOX uptake by reducing the recognition of P-gp. Then, Cur, simultaneously released with DOX from (DOX+Cur)-PMs, has an ability to inhibit P-gp and reduce the efflux of DOX.

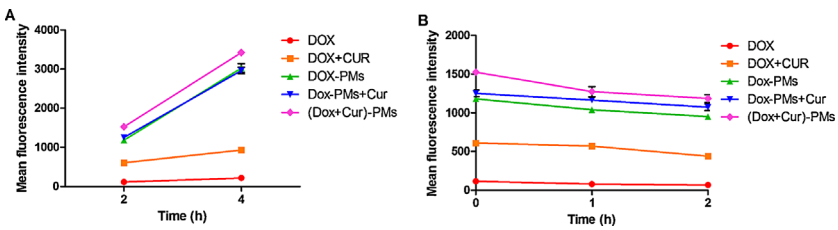

Figure 3. (A) Cellular uptake of DOX in DOX-formulations for 2 h and 4 h in MCF7/Adr cells and (B) efflux of DOX in MCF7/Adr cells after initial incubation 2 h and then replaced with fresh medium for another 1 and 2 h incubation. (n = 3, mean ± SD).

3.5. Apoptosis

In this study, Cur solution or micelles could enhance cellular uptake and cytotoxicity of DOX in MCF7/Adr cells. So cell apoptosis was assayed to evaluate the synergistic effects of Cur or polymeric micelles on DOX. As shown in Figure 6, DOX induced only 4.1% MCF-7/Adr cell apoptosis after 48 h incubation, while Cur had no synergistic effects on cell

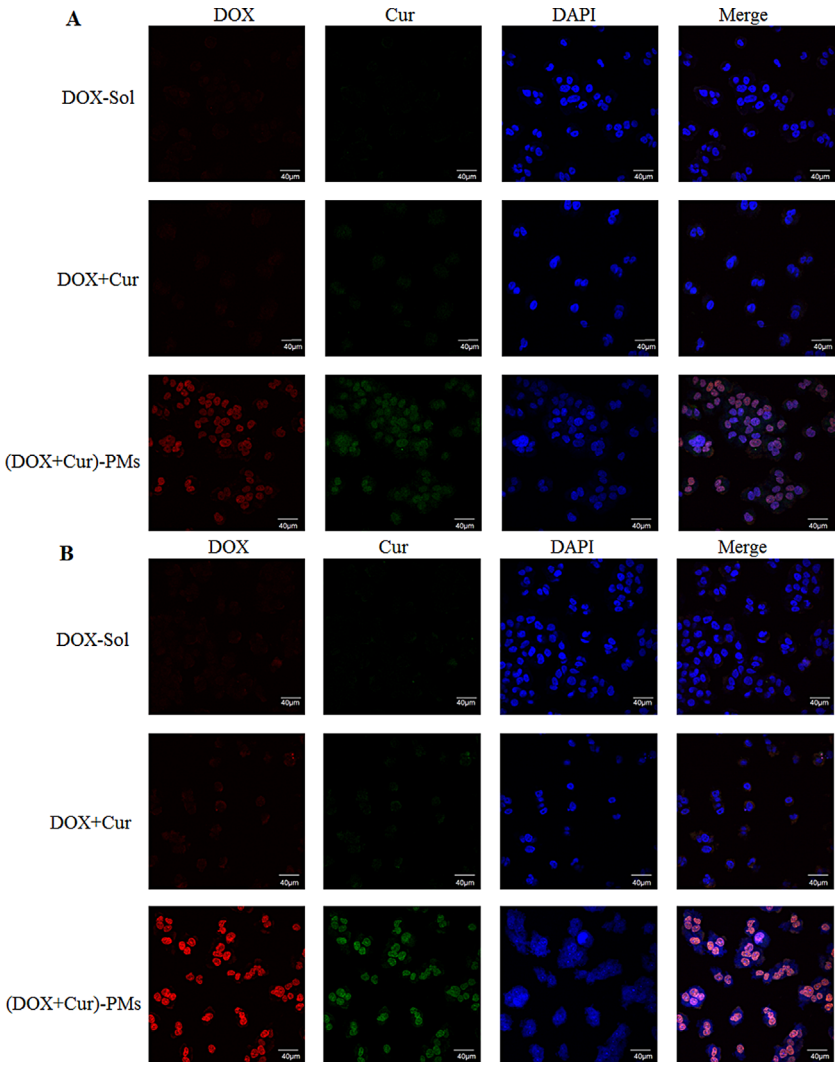

Figure 4. Confocal laser scanning microscopy (CLSM) images of DOX, DOX+Cur and (DOX+Cur)-PMs after incubation with 1 h and 3 h in MCF7/Adr cells, respectively. Scale bar: 40 μm.

apoptosis of DOX. However, DOX-PMs, DOX-PMs+Cur and (DOX+Cur)-PMs induced 48.7%, 49.4% and 74.9% MCF-7/Adr cell apoptosis, respectively, leading to 11.88-, 12.05- and 18.29-fold increase of apoptotic cells compared with DOX-treated cells. It was found that better promotion of apoptosis effect was shown in cells treated with (DOX+Cur)-PMs, compared with that of DOX-PMs and DOX-PMs+Cur. This further proved that co-delivery polymeric micelles could significantly enhance the cytotoxicity, cellular uptake and cell apoptosis of encapsulated drugs, resulting in better antitumor efficacy.

3.6. Pharmacokinetics in Vivo

Mean plasma concentration-time curves of DOX and Cur in rats after intravenous administration of DOX, DOX+Cur, DOX-PMs, DOX-PMs+Cur and (DOX+Cur)-PMs are profiled in Figure 7. The main pharmacokinetic parameters of DOX are listed in Table 1. As shown in Figure 7A, with the addition of Cur, DOX+Cur has the effects of improving the absorption of DOX in vivo. The pharmacokinetic parameter of $AUC_{(0\text{-}t)}$ of DOX+Cur were 1.73-times higher than that of DOX, implying that Cur could increase the absorption of DOX to a certain extent. However, micelles including DOX-PMs, DOX-PMs+Cur and (DOX+Cur)-PMs, resulted in notably increased plasma concentration compared with DOX. Meanwhile, the parameter of area under the curve $(AUC)_{(0\text{-}t)}$ of DOX-PMs, DOX-PMs+Cur and (DOX+Cur)-PMs was 8.34-, 7.78- and 9.38-fold higher than that of DOX-Sol, the mean residence time $(MRT)_{(0\text{-}t)}$ increased 5.44-, 5.82- and 6.32-times, and $t_{1/2}$ was 2.01-, 1.98- and 2.48-fold longer than that of DOX-Sol, suggesting that DOX loaded in micelles could significantly improve blood concentration and prolong blood circulation time of DOX and then have better effects on antitumor efficacy.

The blood concentration of Cur was significantly improved after intravenous administration of (DOX+Cur)-PMs compared with DOX+Cur and DOX-PMs +Cur (shown in Figure 7B). The plasma concentration-time profile and pharmacokinetic parameter of Cur had no differences between DOX+Cur and DOX-PMs+Cur. The $AUC_{(0\text{-}t)}$ of (DOX+Cur)-PMs was 18.46-times higher, $MRT_{(0\text{-}t)}$ 4.38-fold increase, $t_{1/2}$ 7.63-fold increase and clearance (CL) 15.44-fold decrease in comparison with that of DOX+Cur (shown in Table 2). These results were further proof that Cur encapsulated in micelles could extend blood circulation, improve stability and increase plasma concentration of Cur. Therefore, Cur, co-encapsualted with DOX in micelles, could exhibit a good synergistic effect on DOX in vivo.

3.7. In Vivo Antitumor Effect

In vivo antitumor effects of different DOX formulations were carried out in 4T1 bearing Balb/C mice. The tumor volume and body weight of mice were measured every other day and the results were shown in Figure 8. As indicated from Figure 8A, the growth of tumor volume was

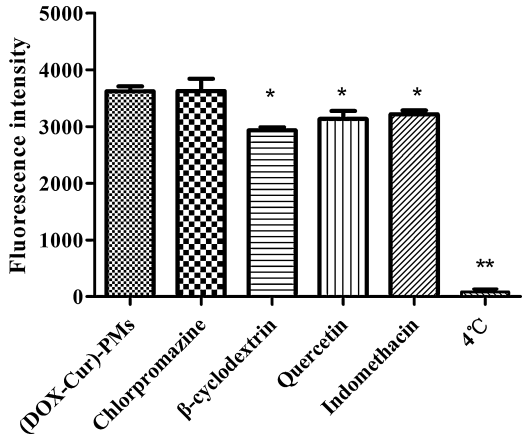

Figure 5. Endocytosis mechanism of (DOX+Cur)-PMs after incubation with different endocytosis inhibitors in MCF7/Adr cells determined by FACS. (n = 3, mean ± SD, *p<0.05, **p<0.01 vs. (DOX+Cur)-PMs).

rapid in saline group. After an injection of DOX and DOX+Cur, tumor volume was significantly decreased compared with saline group. Nevertheless, the growth of tumor volume was obviously reduced in mice treated with DOX-PMs, DOX-PMs+Cur and (DOX+Cur)-PMs compared with single DOX or dual DOX+Cur solution, respectively, which was mainly attributed to long circulation and EPR effects by micelles, and ultimately leading to high accumulation of DOX in tumor sites. In addition, antitumor effects of DOX-Sol or DOX-PMs were not enhanced with the addition of free Cur, indicating that free Cur had no synergistic antitumor efficacy on DOX in vivo, as a result of the instability of Cur in body. However, antitumor efficiency of co-delivery (DOX+Cur)-PMs was more obvious compared with DOX-PMs and DOX-PMs+Cur, which was mainly attributed to the fact that Cur reached the same tumor sites as DOX and played synergistic promotion effects on DOX.

The body weight was monitored every other day and is shown in Figure 8B. Body weight of saline group was increased with time elongation, which was mainly due to the quick growth of tumor volume. However, body weight was significantly decreased after intravenous administration of DOX-Sol and DOX+Cur, because of the systemic toxic effects of DOX. Comparatively, body weights of DOX-PMs, DOX-PMs+Cur and (DOX+Cur)-PMs were not significantly changed, indicating that DOX encapsulated in micelles could reduce systemic side effects. Moreover, almost no weight loss was shown in mice treated with (DOX+Cur)-PMs, indicating that co-delivery of Cur with DOX in micelles could reduce the toxic side-effects of DOX with coordinate efficiency of Cur.

At the end of experiments, tumors were excised and weighed. As seen from Figure 8C and 8D, DOX-PMs, DOX-PMs+Cur and (DOX+Cur)-PMs significantly inhibited tumor growth in comparison with DOX-Sol group ($P < 0.05$ for DOX-PMs and DOX-PMs+Cur, and $P < 0.01$ for

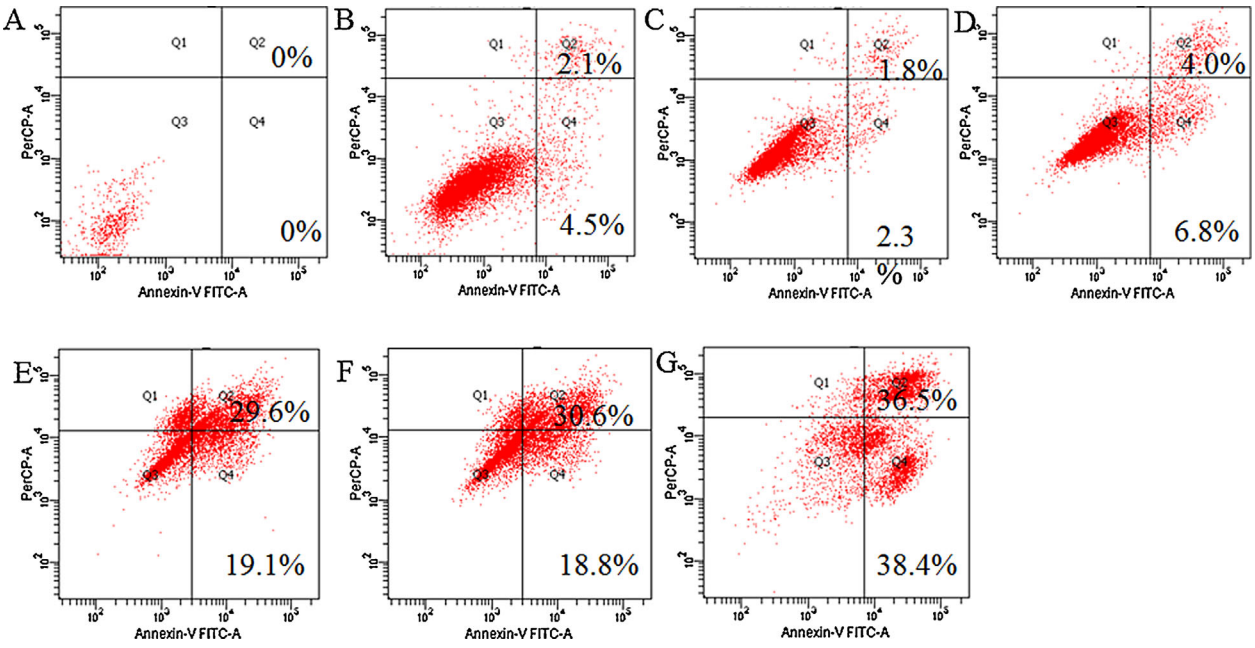

Figure 6. Flow cytometry analysis for apoptosis of (A) blank, (B) Cur, (C) DOX, (D) DOX+Cur, (E) DOX-PMs, (F) DOX-PMs+Cur, (G) (DOX+Cur)-PMs.

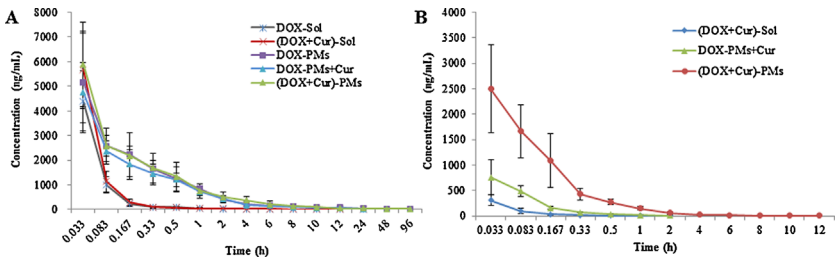

Figure 7. Plasma concentration-time curves of DOX (A) and Cur (B) in rats after intravenous administration of DOX formulations at a dose of 5 mg kg^{-1} DOX and 5 mg kg^{-1} Cur. (n = 5, mean ± SD).

(DOX+Cur)-PMs vs. DOX-Sol). Accordingly, DOX loaded micelles could improve antitumor effects and alleviate adverse side effects of DOX. Furthermore, more remarkable loss of tumor weight was shown in mice treated with (DOX+Cur)-PMs compared with DOX-PMs and DOX-PMs+Cur. In conclusion, co-delivery of DOX and Cur micelles could significantly promote antitumor effects and reduce the side effects of DOX with the synergistic effects of a MDR modulator of Cur.

4. Conclusion

To better overcome MDR, improve antitumor effects and reduce side effects of DOX, polymeric micelles were prepared co-encapsulating DOX and Cur with high encapsulation efficiency and stability. Cur, a chemosensitizer, could increase cellular uptake and improve anticancer efficacy of DOX in MCF7/Adr cells. Meanwhile, co-encapsulating of DOX and Cur in micelles could significantly enhance cellular uptake and apoptosis in vitro, improve antitumor effects and reduce systemic side effects in vivo. Therefore, co-delivery of an anticancer

Table 1. Pharmacokinetic parameters of DOX after intravenous administration of DOX-Sol, (DOX+Cur)-Sol, DOX-PMs, DOX-PMs+Cur, (DOX+Cur)-PMs at a dose of DOX 5 mg kg^{-1} and Cur 5 mg kg^{-1}.

Parameters		DOX-Sol	(DOX+Cur)-Sol	DOX-PMs	DOX-PMs+Cur	(DOX+Cur)-PMs
$AUC_{(0-t)}$	mg L^{-1}h^{-1}	720.37 ± 117.48	1246.82 ± 152.73	6011.51 ± 1031.63	5602.39 ± 816.42	6755.42 ± 1516.175
$AUC_{(0-\infty)}$	mg L^{-1}h^{-1}	815.42 ± 134.85	1314.02 ± 152.19	6333.52 ± 1045.60	6267.17 ± 978.78	7865.025 ± 630.72
$MRT_{(0-t)}$	h	2.72 ± 1.14	15.66 ± 2.53	14.80 ± 3.05	15.82 ± 3.00	17.18 ± 2.94
$MRT_{(0-\infty)}$	h	7.44 ± 5.69	20.42 ± 5.00	21.11 ± 8.24	23.49 ± 5.85	47.20 ± 41.38
$t_{1/2}$	h	12.05 ± 6.17	22.92 ± 5.72	24.23 ± 9.51	23.84 ± 7.03	29.87 ± 10.60
t_{max}	h	0.03	0.03	0.03	0.03	0.03
CLz	L h^{-1}kg^{-1}	6.28 ± 1.16	0.00	0.81 ± 0.14	0.93 ± 0.24	0.00
Vz	L kg^{-1}	103.41 ± 49.27	0.13 ± 0.03	28.12 ± 12.39	35.69 ± 11.78	0.05 ± 0.04
C_{max}	mg L	4398 ± 1084.61	5488.33 ± 1629.27	5166 ± 1984.12	4958 ± 1237.99	5888 ± 1697.16

Table 2. Pharmacokinetic parameters of Cur after intravenous administration of (DOX+Cur)-Sol, DOX-PMs+Cur, (DOX+Cur)-PMs at a dose of DOX 5 mg kg^{-1} and Cur 5 mg kg^{-1}.

Parameters		(DOX+Cur)-Sol	DOX-PMs+Cur	(DOX+Cur)-PMs
AUC(0-t)	mg L^{-1}h^{-1}	45.89 ± 7.37	99.93 ± 53.07	846.97 ± 174.25
AUC(0-∞)	mg L^{-1}h^{-1}	46.86 ± 7.82	102.96 ± 55.21	864.74 ± 178.74
MRT(0-t)	h	0.26 ± 0.09	0.27 ± 0.06	1.14 ± 0.27
MRT(0-∞)	h	0.31 ± 0.09	0.35 ± 0.11	1.50 ± 0.61
$t_{1/2z}$	h	0.46 ± 0.18	0.52 ± 0.18	3.51 ± 1.73
t_{max}	h	0.03	0.03	0.03
CLz	L h^{-1}kg^{-1}	105.15 ± 16.91	68.90 ± 29.53	6.08 ± 1.76
Vz	L kg^{-1}	71.62 ± 23.37	50.46 ± 37.03	30.08 ± 13.54
C_{max}	mg L^{-1}	341.50 ± 58.28	581.33 ± 321.50	2496.67 ± 861.85

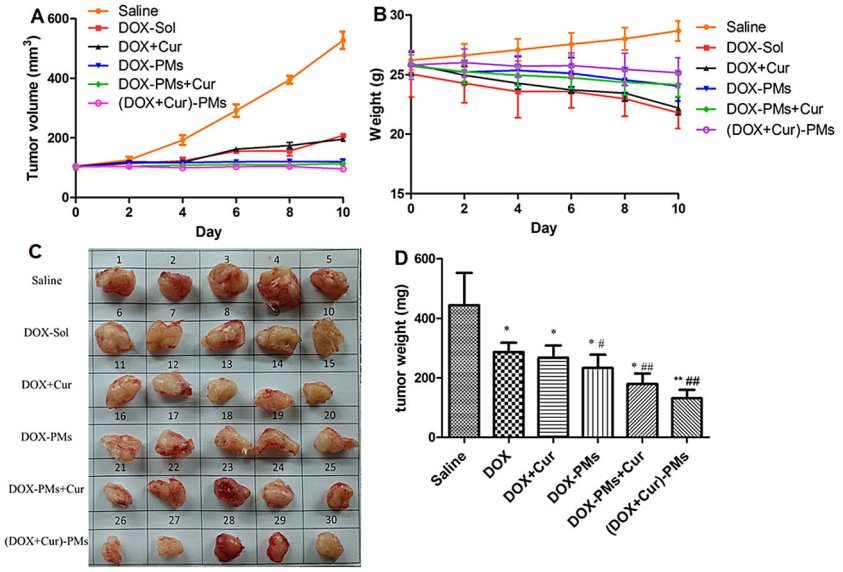

Figure 8. The antitumor effects of DOX formulations on 4T1-bearing mice after intravenous administration with saline, DOX, DOX+Cur, DOX-PMs, DOX-PMs+Cur, (DOX+Cur)-PMs. (A) Tumor growth inhibition efficacy and (B) The changes of mice weight after i.v. injection of different formulations on day 1, 4, 7 at a dose of 10 mg DOX kg^{-1}. (C) Representative excised tumor from the sacrificed mice at day 10. (D) Weight of separated tumors from sacrificed mice ($n = 6$, mean ± SD, $^{*}P<0.05$, $^{**}P<0.01$ vs. saline group, $^{\#}P<0.05$, $^{\#\#}P<0.01$ vs. DOX group.)

agent and chemosensitizer might be a promising vehicle for tumor therapy.

Acknowledgements: Specialized Research Fund for the Doctoral Program of Higher Education (20130013120008) and Youth Foundation of Beijing University of Chinese Medicine (2013-QNJSZX024) are gratefully acknowledged for financial support.

Received: February 7, 2015; Accepted: April 16, 2015;Published online: May 15, 2015; DOI: 10.1002/mabi.201500043

Keywords: antitumor; co-delivery; curcumin; doxorubicin; polymeric micelles

[1] B. Ma, S. Chai, N. Li, K. K. To, W. L. Kan, D. Yang, G. Lin, *Int. J. Pharm.* **2012**, *424*, 33.
[2] A. H. Schinkel, J. W. Jonker, *Adv. Drug Delivery Rev.* **2003**, *55*, 3.
[3] D. Pramanik, N. R. Campbell, S. Das, S. Gupta, V. Chenna, S. Bisht, P. Sysa-Shah, D. Bedja, C. Karikari, C. Steenbergen, K. L. Gabrielson, A. Maitra, A. Maitra, *Oncotarget* **2012**, *3*, 640.
[4] H. Qian, Y. Yang, X. Wang, *Eur. J. Pharm. Sci.* **2011**, *43*, 125.
[5] B. H. Choi, C. G. Kim, Y. Lim, S. Y. Shin, Y. H. Lee, *Cancer Lett.* **2008**, *259*, 111.
[6] S. Shukla, H. Zaher, A. Hartz, B. Bauer, J. A. Ware, S. V. Ambudkar, *Pharm. Res.* **2009**, *26*, 480.
[7] E. Meiyanto, D. D. Putri, R. A. Susidarti, R. Murwanti, Sardjiman, A. Fitriasari, U. Husnaa, H. Purnomo, M. Kawaichi, *Asian Pac. J. Cancer Prev.* **2014**, *15*, 179.
[8] A. M. Chuah, B. Jacob, Z. Jie, S. Ramesh, S. Mandal, J. K. Puthan, P. Deshpande, V. V. Vaidyanathan, R. W. Gelling, G. Patel, T. S. Shreeram, *Food Chem.* **2014**, *156*, 227.
[9] T. H. Chen, Y. C. Yang, J. C. Wang, J. J. Wang, *Transplant. Proc.* **2013**, *45*, 3546.
[10] C. Yang, K. Wu, S. H. Li, Q. You, *Pharm. Biol.* **2013**, *51*, 482.
[11] J. Duan, H. M. Mansour, Y. Zhang, X. Deng, Y. Chen, J. Wang, Y. Pan, J. Zhao *Int. J. Pharm.* **2012**, *426*, 193.
[12] R. Misra, S. K. Sahoo, *Mol. Pharm.* **2011**, *8*, 852.
[13] B. L. Wang, Y. M. Shen, Q. W. Zhang, Y. L. Li, M. Luo, Z. Liu, Y. Li, Z. Y. Qian, X. Gao, H. S. Shi, *Int. J. Nanomed.* **2013**, *8*, 3521.
[14] Q. Guo, X. Li, Y. Yang, J. Wei, Q. Zhao, F. Luo, Z. Qian, *J. Biomed. Nanotechnol.* **2014**, *10*, 227.
[15] S. Barui, S. Saha, G. Mondal, S. Haseena, A. Chaudhuri, *Biomaterials* **2014**, *35*, 1643.
[16] X. B. Xiong, A. Falamarzian, S. M. Garg, A. Lavasanifar, *J. Controlled Release* **2011**, *155*, 248.
[17] X. Wang, Y. Chen, F. Z. Dahmani, L. Yin, J. Zhou, J. Yao, *Biomaterials* **2014**, *35*, 7654.
[18] Z. Zhang, S. Tan, S. S. Feng, *Biomaterials* **2012**, *33*, 4889.
[19] G. Cornaire, J. Woodley, P. Hermann, A. Cloarec, C. Arellano, G. Houin, *Int. J. Pharm.* **2004**, *278*, 119.
[20] H. J. Youk, E. Lee, M. K. Choi, Y. J. Lee, J. H. Chung, S. H. Kim, C. H. Lee, S. J. Lim, *J. Controlled Release* **2005**, *107*, 43.
[21] J. Wang, J. Sun, Q. Chen, Y. Gao, L. Li, H. Li, D. Leng, Y. Wang, Y. Sun, Y. Jing, S. Wang, Z. He, *Biomaterials*, **2012**, *33*, 6877.
[22] F. Mathot, A. des Rieux, A. Arien, Y. J. Schneider, M. Brewster, V. Preat, *J. Controlled Release* **2007**, *124*, 134.
[23] B. He, Z. Jia, W. Du, C. Yu, Y. Fan, W. Dai, L. Yuan, H. Zhang, X. Wang, J. Wang, X. Zhang, Q. Zhang, *Biomaterials* **2013**, *34*, 4309.
[24] R. Mo, X. Jin, N. Li, C. Ju, M. Sun, C. Zhang, Q. Ping, *Biomaterials* **2011**, *32*, 4609.